

Preparation of Hybrid NiO-Graphene Quantum Dots for Electrochemical Sensing of Dopamine

Doğa Bahçeci

CHEM401 GRADUATION PROJECT
in
Chemistry

Eastern Mediterranean University
June 2023
Gazimağusa, North Cyprus

Approval of the Department of Chemistry

I certify that this report satisfies all the requirements as a CHEM401 Graduation Project report for the degree of Bachelor of Science in Chemistry.

Prof. Dr. İzzet Sakallı
Chair, Department of Chemistry

We certify that we have read this thesis and that in our opinion it is fully adequate in scope and quality as a CHEM401 Graduation Project report for the degree of Bachelor of Science in Chemistry.



Assoc. Prof. Dr. Akeem Oladipo
Co- Supervisor



Prof. Dr. Mustafa Gazi
Supervisor

Prof. Dr. Huriye İcil
CHEM401 Graduation Project Coordinator

ABSTRACT

Dopamine is a neurotransmitter responsible for mood regulation, muscle movement, and wakefulness cycle. Abnormal dopamine levels lead serious disorders like Parkinson's Disease, depression, or cardiovascular diseases. Correct detection of dopamine is important for diagnosis and treatment of dopamine related disorders. Electrochemical sensors gained a great interest in the research field in recent years due to their simplicity, low cost, and sensitivity. In the current study, hybrid dopamine electrochemical sensor is developed for the quantification of dopamine. NiO nanoparticles and graphene quantum dots were used in hybrid structure. The results demonstrate that the hybrid dopamine sensor has higher conductivity and sensitivity rather than the sensors that are developed with one material.

Keywords: dopamine, electrochemistry, electrochemical sensors, green synthesis.

ÖZ

Dopamin, mod düzenlemesi, kas hareketi ve uyanıklık döngüsünden sorumlu bir nörotransmitterdir. Anormal dopamin seviyeleri, Parkinson Hastalığı, depresyon veya kardiyovasküler hastalıklar gibi ciddi rahatsızlıklara yol açar. Dopaminin doğru saptanması, dopamine bağlı bozuklukların tanı ve tedavisi için önemlidir. Elektrokimyasal sensörler, basitliği, düşük maliyeti ve hassasiyeti nedeniyle son yıllarda araştırma alanında büyük ilgi görmüştür. Mevcut çalışmada, dopamin miktarının belirlenmesi için hibrit dopamin elektrokimyasal sensörü geliştirilmiştir. Hibrit yapıda NiO nanoparçacıkları ve grafen kuantum noktaları kullanılmıştır. Sonuçlar, hibrit dopamin sensörünün tek malzeme ile geliştirilen sensörlere göre daha yüksek iletkenliğe ve duyarlılığa sahip olduğunu göstermektedir.

Anahtar Kelimeler: dopamine, elektrokimya, elektrokimyasal sensörler, yeşil sentez.

ACKNOWLEDGMENT

I would like to acknowledge and give my thanks to Assoc Prof.Dr. Akeem Adeyemi Oladipo and Prof.Dr. Mustafa Gazi for their supervision, advice, and guidance from the very early stages of this thesis.

TABLE OF CONTENTS

ABSTRACT.....	ii
ÖZ.....	iii
ACKNOWLEDGMENT.....	iv
TABLE OF CONTENTS.....	v
LIST OF TABLES.....	ix
LIST OF FIGURES.....	x
LIST OF SYMBOLS AND ABBREVIATIONS.....	xii
INTRODUCTION.....	1
1.1 Dopamine.....	1
1.1.1 Dopamine Chemical Structure.....	1
1.1.2 Catecholamine Biosynthesis.....	2
1.1.3 Distribution of Dopamine in the human body.....	3
1.1.4 Role of Dopamine in Diseases.....	4
1.2 Dopamine Detection Technologies.....	5
1.2.1 High-performance Liquid Chromatography.....	5
1.2.2 Enzyme-linked immunosorbent assay.....	5

1.2.3 Chemiluminescence	6
1.2.4 Fluorescence Spectroscopy	6
1.2.5 Capillary electrophoresis.....	6
1.2.6 Surface enhanced Raman spectroscopy	7
1.2.7 Electrochemical Sensors	7
1.3 Thesis objectives	7
1.4 Thesis Limitations.....	7
LITERATURE REVIEW	8
2.1 Enzyme-linked immunosorbent assay (ELISA.....	8
2.1.1 Basic Principles of Enzyme-linked immunosorbent assay	8
2.1.2 Types of Enzyme-linked immunosorbent assay	9
2.1.3 Advantages of competitive ELISA	10
2.1.4 Disadvantages of competitive ELISA.....	10
2.1.5 ELISA in dopamine detection.....	11
2.2 Fluorescence Spectroscopy	11
2.2.1 Basic Principles of Fluorescence Spectroscopy.....	12
2.2.2 Advantages of Fluorescence spectroscopy	12
2.2.3 Disadvantages of Fluorescence spectroscopy	13
2.2.4 Fluorescence spectroscopy in dopamine detection	13

2.3 High-performance Liquid Chromatography	13
2.3.1 Basic Principles of HPLC	14
2.3.2 Advantages of HPLC	14
2.3.3 Disadvantages of HPLC.....	15
2.3.4 HPLC Method in Dopamine Detection.....	15
2.4 Portable sensors	15
2.5 Working principles of electrochemical sensors	16
2.6 Electrochemical Sensors for Dopamine Detection	18
EXPERIMENTAL STUDY	25
3.1 Reagents and Materials	25
3.2 Experimental	25
3.2.1 Synthesis of Graphene Quantum Dots	25
3.2.2 Synthesis of NiO Nanoparticles	26
3.2.3 Synthesis of Hybrid Quantum Dots	27
3.2.4 Characterization	28
3.2.5 Preparation of Ferrocyanide and Sodium Sulphate Stock Solutions	28
3.2.6 Modified Electrode Fabrication and Preparation	28
3.2.7 Preparation of Phosphate-buffered Saline Solution	30
3.2.8 Preparation of Dopamine Solutions	30

3.2.9 Preparation of Real Samples	30
3.3 Electrochemical Test.....	30
RESULTS AND DISCUSSIONS.....	36
4.1 FTIR Analysis Results	36
4.2 Electroactive Surface Area of Materials in Ferrocyanide	38
4.3 EIS Results of Materials in Ferrocyanide	40
4.4 Calibration Curve.....	41
4.5 Limit of Detection and Limit of Quantification Calculations.....	41
4.6 Relative Standard Deviation Calculations	42
4.7 Stability studies.....	44
4.8 Results of Selectivity Studies.....	44
4.9 Amperometry results.....	45
4.10 Discussion	45
CONCLUSION.....	47
REFERENCES	48

LIST OF TABLES

Table 1: Electroactive surface area results.....	39
Table 2: EIS results depending on the diagram above.....	40
Table 3: RSD results	42
Table 4: RSD results of blood sample	42
Table 5: RSD results of serum sample.....	43
Table 6: RSD results of urine sample	43

LIST OF FIGURES

Figure 1: Dopamine Structure (PubChem, n.d.)	1
Figure 2: Dopamine Synthesis in neuron (Berends et al., 2019)	3
Figure 3: Distribution of dopamine in periphery: dashed lines show dopamine receptors and continuous lines show dopamine expression locations. (Klein et al., 2018).....	4
Figure 4: ELISA types (Anagu & Andoh, 2022)	9
Figure 5: Fluorescence spectroscopy components (Zacharioudaki et al., 2022)	12
Figure 6: HPLC components (Lozano-Sánchez et al., 2018)	14
Figure 7: Biosensor setup (Ramesh et al., 2022)	15
Figure 8: Reference electrode (Ag/AgCl Reference Electrode Silver Silver Chloride, n.d.)	17
Figure 9: Counter electrode (Counter Electrode Low Price Auxiliary Electrode, n.d.).	18
Figure 10: Working electrode (Platinum Disc Working Electrode 99.99% Purity, n.d.)	18
Figure 11: Graphene Quantum Dots under UV light.....	26
Figure 12: Coated electrode	29
Figure 13: Three-electrode system with ferrocyanide	31
Figure 14: Diluted blood sample.....	34
Figure 15: FTIR of 1-hybrid	36
Figure 16: FTIR of 2-hybrid	37

Figure 17: FTIR of 3-hybrid	37
Figure 18: CVs of (a)1-hybrid (b) 2-hybrid (c) 3-hybrid.....	38
Figure 19: EIS diagram.....	40
Figure 20: Calibration Curve	41
Figure 21: CV results of stability studies.....	44
Figure 22: Selectivity results (a)DPV (b)CV	45
Figure 23: Amperometry results	45

LIST OF SYMBOLS AND ABBREVIATIONS

AA	Ascorbic Acid
ATR-FTIR	Attenuated Total Reflection Fourier Transform Infrared Spectroscopy
CA	Citric Acid
CV	Cyclic Voltammetry
DPV	Differential Pulse Voltammetry
DA	Dopamine
EDX	EDAX TEAM Energy Dispersive X-Ray
EIS	Electrochemical Impedance Spectroscopy
ELISA	Enzyme-Linked Immunosorbent Assay
FESEM	Field Emission Scanning Electron Microscopy
FTIR	Fourier Transformed Infrared Spectroscopy
Gqds	Graphene Quantum Dots

HPLC	High Performance Liquid Chromatography
HRTEM	High-Resolution Transmission Electron Microscopy
LOD	Limit Of Detection
LOQ	Limit Of Quantification
LSV	Linear Sweep Voltammetry
SEM	Scanning Electron Microscopy
TGA	Thermogravimetric Analysis
TEM	Transmission Electron Microscopy (TEM)
UA	Uric Acid
XRD	X-Ray Diffraction
XPS	X-Ray Photoelectron Spectroscopy (XPS)

Chapter 1

INTRODUCTION

1.1 Dopamine

In nervous system, signalling molecules that is released to the synaptic cleft from axon terminal and binds to the receptors of the postsynaptic cell to continue action potential along the neuron are called neurotransmitters. The molecular identity of neurotransmitters differs (peptides, amino acids, organic molecules, nucleotides, or monoamines) (Klein et al., 2018). Interestingly, monoamines participate in regulating homeostasis by acting like a hormone (regulatory molecules). Catecholamines are a kind of monoamine that contain catechol group in addition to the amine group. Epinephrine, norepinephrine, and dopamine are the most common examples of catecholamines. These three neurotransmitters are secreted via adrenal gland to keep body homeostasis (Franco et al., 2021; Klein et al., 2018).

1.1.1 Dopamine Chemical Structure

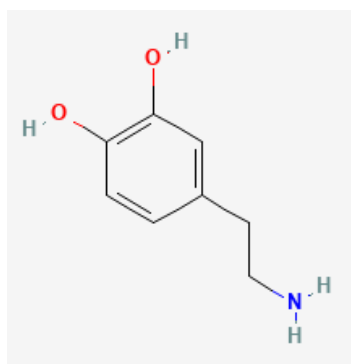


Figure 1: Dopamine Structure (PubChem, n.d.)

The catecholamine, dopamine has a molecular formula of $C_8H_{11}NO_2$. IUPAC name of the dopamine is 4-(2-aminoethyl) benzene-1,2-diol. As can be seen in the figure above dopamine is composed of one two hydroxyl groups and an ethyl group with ammine group attached to the benzene ring (PubChem, n.d.).

1.1.2 Catecholamine Biosynthesis

Catecholamine biosynthesis occurs in various steps and all dopamine, adrenaline, and noradrenaline are derived from amino acids phenylalanine and/or tyrosine. These three catecholamines are produced in the same biosynthesis metabolism. The product depends on the enzyme expression in the cell. Tyrosine can be taken directly via diet or produced from essential amino acid phenylalanine by phenylalanine hydroxylase. Tyrosine is then converted to levodopa (L-3,4-dihydroxyphenylalanine or L-DOPA) by tyrosine hydroxylase and levodopa is converted to dopamine with the help of enzyme L- aromatic amino acid decarboxylase (AADC). Dopamine β -hydroxylase (DBH) catalyses dopamine to norepinephrine. Epinephrine is produced by the catalysation of norepinephrine via phenyl ethanolamine-N-methyltransferase (PNMT) (Berends et al., 2019).

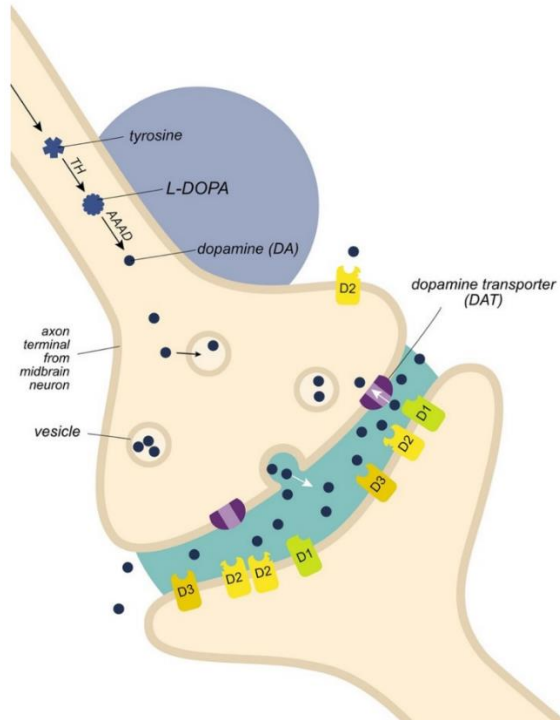


Figure 2: Dopamine Synthesis in neuron (Berends et al., 2019)

1.1.3 Distribution of Dopamine in the human body

Dopamine regulates mood, movement of muscles, and wakefulness cycle. Due to its crucial functions, dopamine is distributed around the whole body. In addition to the brain, dopamine is expressed in kidneys and the gut. Most of the dopamine receptors are located in the brain while the rest are distributed to retina, heart, blood veins, adrenal gland, and kidneys (Chatterjee et al., 2022; Fernandez-Chiappe et al., 2020; Klein et al., 2018).

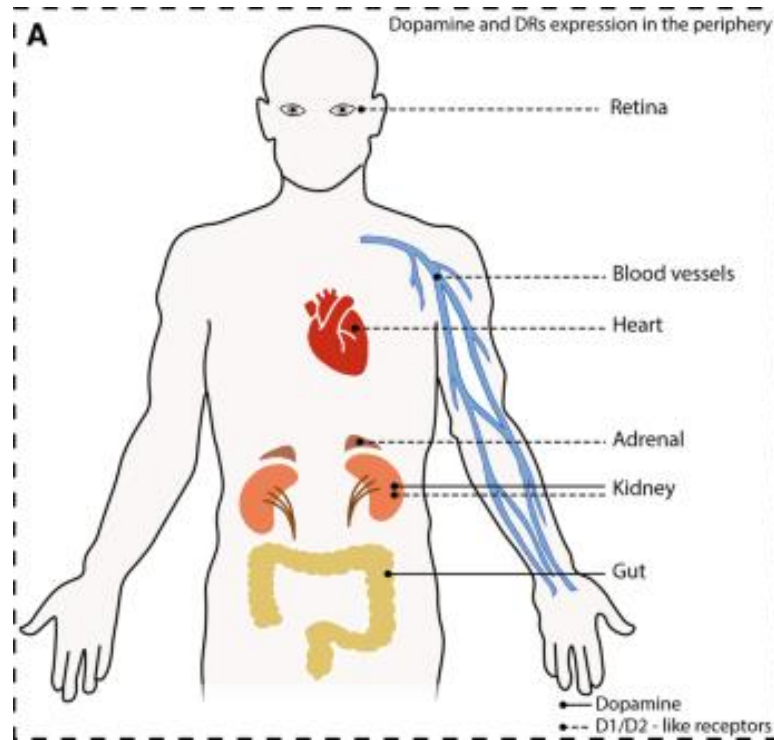


Figure 3: Distribution of dopamine in periphery: dashed lines show dopamine receptors and continuous lines show dopamine expression locations. (Klein et al., 2018)

1.1.4 Role of Dopamine in Diseases

Dysfunction of dopamine leads to several severe diseases. For instance, high levels of dopamine are associated with cardiovascular system disorders while low levels of dopamine are associated with neurological disorders such as Parkinson's disease, schizophrenia, and depression (Chatterjee et al., 2022; Lakard et al., 2021; Arumugasamy et al., 2020; Klein et al., 2018).

1.2 Dopamine Detection Technologies

Dopamine presents in the treatment and diagnosis of many diseases (mainly neurodegenerative disorders). Because of its importance in therapy and diagnosis, the detection of dopamine is crucial for researchers. High-performance liquid chromatography (HPLC), chemiluminescence, surface-enhanced Raman spectroscopy, capillary electrophoresis, ELISA, fluorescence spectroscopy, and electrochemical sensors are some of the methods that is used in dopamine detection (Ferry et al., 2014).

1.2.1 High-performance Liquid Chromatography

High-performance liquid chromatography (HPLC) is a column chromatography technique that high performance pump pumps pressure to the column with stationary phase. The retention time of analyte in mobile phase is detected and a signal is generated for quantification. HPLC is one of the most common dopamine detection methods due to its speed. Faster movement in the column indicates lower affinity (Petrova & Sauer, 2017).

1.2.2 Enzyme-linked immunosorbent assay

Enzyme-linked immunosorbent assay (ELISA) is a technique that is used to detect antigens in biological fluids using antibodies. Among the four types of ELISA, competitive ELISA is used in dopamine detection. This type of ELISA is used for concentration detections. Due to the low concentration of catecholamines in the body fluids highly sensitive antibodies are used. In this method, the targeted antibody (anti-dopamine antibody) is fixed to the bottom of the well. Next, the specimen and

enzyme-conjugated antigen (dopamine) was added to the well. Colour change has not been noticed as a result of antigen antibody interaction in case of dopamine presence (Alhajj & Farhana, 2020; Kim et al., 2008).

1.2.3 Chemiluminescence

A chemical reaction resulting with the emission of light is called chemiluminescence. Chemiluminescence is an immunoassay technique that is used in molecule determination like hormones, proteins, or nucleic acids. Chemiluminescence can be both direct (luminophore markers) and indirect (enzyme markers) (Cinquanta et al., 2017). In 2019, Lan et al. utilized lucigenin-riboflavin chemiluminescence for dopamine detection (Lan et al., 2019).

1.2.4 Fluorescence Spectroscopy

Fluorescence spectroscopy is a technique based on photon emission after excitation by absorbance of the light. As the name suggests, fluorescence spectroscopy analyses photoluminescence, fluorescence (Zacharioudaki et al., 2022).

1.2.5 Capillary electrophoresis

Molecules are separated depending on their sizes and charges in capillary electrophoresis. Fang et al., and Claude et al. used capillary electrophoresis for dopamine detection (Fang et al., 2013; Claude et al., 2011).

1.2.6 Surface enhanced Raman spectroscopy

Surface enhanced Raman spectroscopy (SERS) is a technique that is used in the presence of biomolecules with enhanced signal intensity. Nanoprobes are used in SERS. In 2015, An et al., used SERS method to detect dopamine level of 1-methyl-4-phenyl-1, 2, 3, 6-tetrahydropyridine (MPTP) injected and non-injected mouse models (An et al., 2015).

1.2.7 Electrochemical Sensors

Electrochemical sensors have gained a great interest in recent years due to their low-cost, reliability, and specificity. In these sensors, quantity of the sample is detected by electrodes and can be read with a device called potentiostat. In dopamine detection, biosensors developed from different materials are commonly used.

1.3 Thesis objectives

The following is the goal of this thesis:

- ❖ To develop a hybrid dopamine sensor with enhanced conductivity and sensitivity.

1.4 Thesis Limitations

The following is this work's limitation:

- ❖ Due to the equipment problem, the effect of pH to the hybrid sensor could not be detected.

Chapter 2

LITERATURE REVIEW

2.1 Enzyme-linked immunosorbent assay (ELISA)

In radioimmunoassay, tagged antibodies and antigens were conjugated with enzymes and not radioactive iodine. This modification was resulted in the invention of ELISA technique. Enzyme-linked immunosorbent assay is a quantitative assay to detect specific components (hormones, proteins, and antibodies) in biological samples. In general, target antigen detection was done by the antigen-specific antibodies. Antigen presence can be detected by the colour change of the solution. Nowadays, ELISA is used in cytokine and receptor measurements, pregnancy tests and diagnostics (Alhajj & Farhana, 2020; Horlock, n.d.).

2.1.1 Basic Principles of Enzyme-linked immunosorbent assay

ELISA is usually performed in 96 well plates and has four general steps. In the first step, antigen or antibody is fixed to the bottom of the well. Magnetic particles and plastic beads can be listed as solid surfaces for coating instead of microtiter well. In the next step, blocking buffer (i.e., Bovine serum albumin (BSA)) is added to block unoccupied plate surface. In the third step, enzyme-linked antibody detects the relevant antigen. The final step is to measure the results. Washing of the well with buffer is done between each step (Alhajj & Farhana, 2020).

2.1.2 Types of Enzyme-linked immunosorbent assay

There are four types of ELISA: direct, indirect, sandwich, and competitive ELISA.

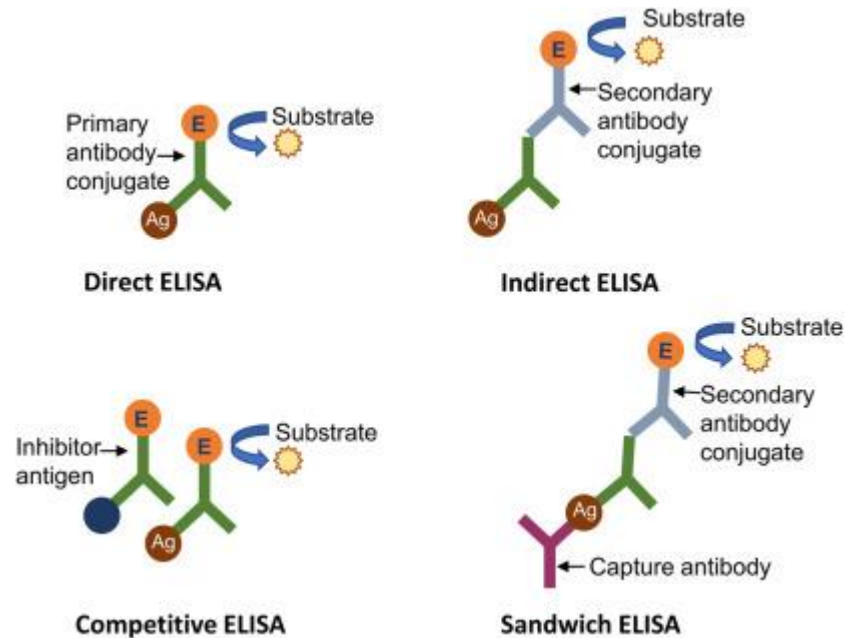


Figure 4: ELISA types (Anagu & Andoh, 2022)

In the direct ELISA method, antigen is coated to the bottom of the well and enzyme-linked antibody binds the antigen directly (Alhajj & Farhana, 2020).

In the indirect ELISA method, again antigen is coated to the bottom of the well. Primary antibody binds to the relevant antigen in the surface and enzyme-linked antibody binds to the primary antibody (Alhajj & Farhana, 2020).

In the sandwich ELISA method, antibody that antigen binds is coated to the bottom of the well. Another antibody which is enzyme linked, binds to the same antigen (Alhajj & Farhana, 2020).

In competitive ELISA method, antibody is coated to the bottom of the well. Specimen and reagent (which is enzyme conjugated antigen) are added to the well. Antigens in the sample compete with the reagent antigens to bind the antibodies coated in the surface. The only washing step of this ELISA method is after antigen-antibody binding. Different than the other ELISA methods colour change is inversely proportional to the concentration of antigen. If more reagent binds to the antibodies deeper colour will be obtained. That means the antigen of interest is low in the specimen. Competitive ELISA method is used in dopamine detection (Alhajj & Farhana, 2020; Kim et al., 2008).

2.1.3 Advantages of competitive ELISA

1. Sample purification is needed less.
2. Range of antigens it can measure is large.
3. Low-cost

2.1.4 Disadvantages of competitive ELISA

1. Specificity is low.
2. It cannot be used in diluted samples.
3. Variability is low.
4. It can only be used for small antigens.

2.1.5 ELISA in dopamine detection

There are some experiments that used the ELISA method to detect dopamine.

Nichkova et al. determined dopamine in urine using competitive ELISA in 2013. This experiment was done to check the effect of different treatment methods in Parkinson's disease patients. The results were accurate and precise. The authors suggested that the competitive ELISA can be used for monitoring the effect of dopamine treatment (Nichkova et al., 2013).

Sethu et al. checked dopamine levels in plasma and tear using competitive ELISA in 2019. The lower level of dopamine was detected in plasma than the tear fluid (Sethu et al., 2019).

2.2 Fluorescence Spectroscopy

Fluorescence is the emission of photon that occurs after the excitation of a substance that absorbs light. Fluorescence is analyzed by electromagnetic spectroscopy method, fluorescence spectroscopy (Zacharioudaki et al., 2022; Shahzad et al., 2009).

2.2.1 Basic Principles of Fluorescence Spectroscopy

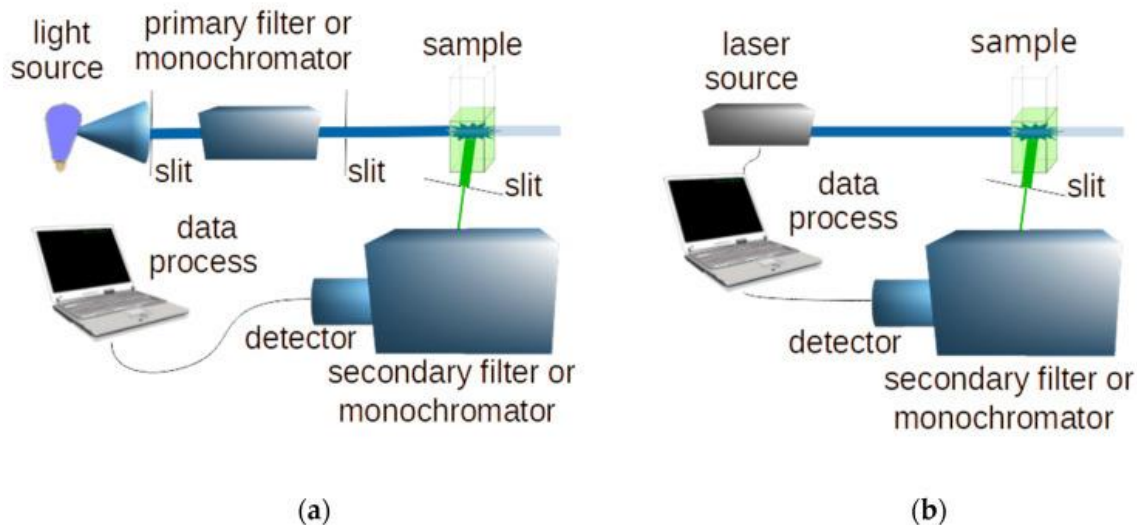


Figure 5: Fluorescence spectroscopy components (Zacharioudaki et al., 2022)

Fluorescence spectroscopy composed of light, monochromator (excitation and emission), chamber to put the target material, and detector. The laser-induced fluorescence spectroscopy has laser instead of light source. The light or laser source passes through monochromator (excitation), then reaches to the sample holder, again monochromator (emission one) and detector detects the fluorescence (Zacharioudaki et al., 2022; Shahzad et al., 2009).

2.2.2 Advantages of Fluorescence spectroscopy

1. High sensitivity
2. High specificity
3. Fluorescence spectroscopy can identify very low concentrations of molecules.
4. Time of decay, and intensity to fluorescence is measurable.

2.2.3 Disadvantages of Fluorescence spectroscopy

1. Fluorophores have a short lifetime.
2. Hence, all molecules do not have fluorescence, fluorescence spectroscopy cannot be used.
3. It is very sensitive to oxygen and pH.
4. Toxicity.

2.2.4 Fluorescence spectroscopy in dopamine detection

In 2022, Zakaria et al. developed nanocapsules for the detection of dopamine via fluorescence spectroscopy. Nanocapsules are usually formed for drug entrapment to reach the target. An anti-inflammatory and an antioxidant drug called curcumin is used in the material detection. For instance, curcumin was combined with poly (dimethyldiallylammonium chloride) (PDDA) for ATP detection. In this experiment, Zakaria et al. combined curcumin with poly lactic-co-glycolic acid (PLGA) and PDDA. Hybrid nanocapsules were mixed with different concentrated dopamine solutions. Fluorescence spectroscopy was performed. In conclusion, nanocapsules were successful to detect dopamine up to 5mM (Zakaria et al., 2022).

2.3 High-performance Liquid Chromatography

A type of column chromatography method that uses high-pressure pump is called high-performance liquid chromatography (Petrova & Sauer, 2017).

2.3.1 Basic Principles of HPLC

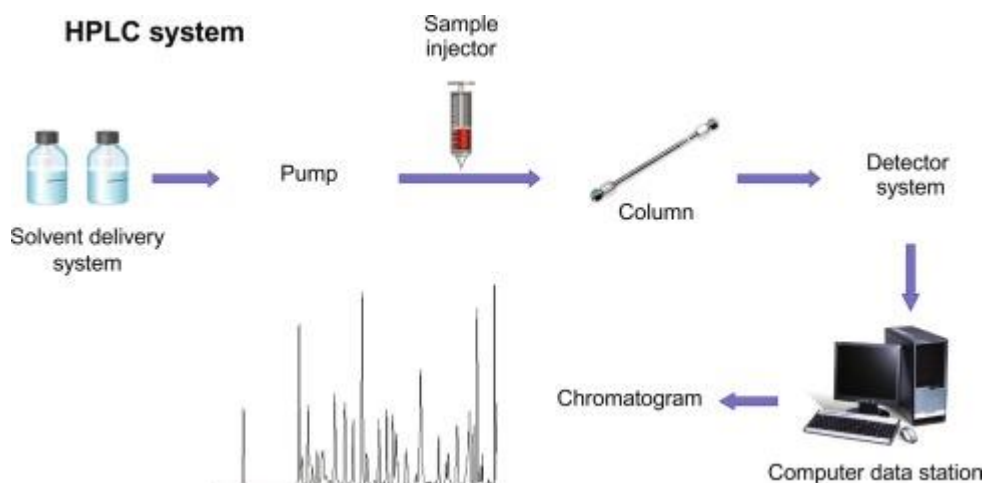


Figure 6: HPLC components (Lozano-Sánchez et al., 2018)

HPLC is based on the dissolution of sample in solvent (mobile phase). There are six components in the setup of HPLC: column, high-performance pump, detector, sample injector, solvent and data station. First the stationary phase is prepared in column using silica or cellulose. Next, the sample is injected to the column with the help of pump in a constant flow rate. Then, mobile phase (solvent) passes through for the detection of absorption. The speed of sample is detected by detector and send to the computer (Lozano-Sánchez et al., 2018).

2.3.2 Advantages of HPLC

1. High sensitivity.
2. HPLC is precise.
3. Speed.
4. Accurate.
5. High reproducibility.

2.3.3 Disadvantages of HPLC

1. Only dissolved samples can be detected.
2. Expensive
3. Complex.
4. Low sensitivity.

2.3.4 HPLC Method in Dopamine Detection

High-performance liquid chromatography is widely used in dopamine detection. For example, in 2020, HPLC method was developed to detect dopamine HCl in injectable solutions. HPLC detected the dopamine successfully (Aydin & Bulduk, 2020).

2.4 Portable sensors

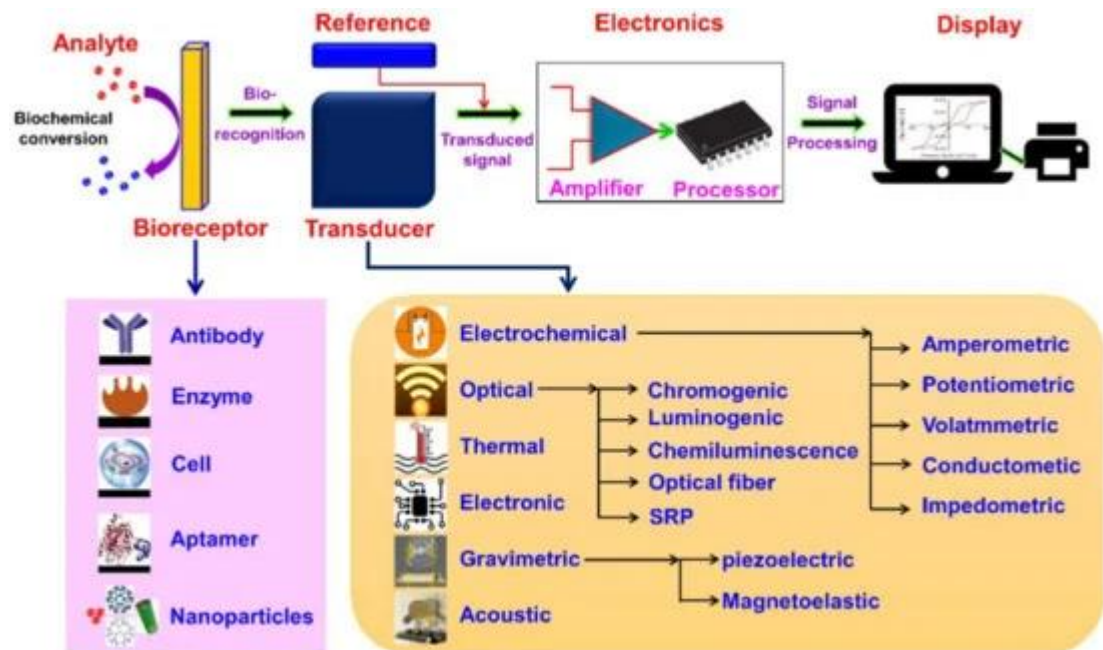


Figure 7: Biosensor setup (Ramesh et al., 2022)

Electrochemical detection of biological events like antigen antibody interaction can be done using electrochemical biosensors. Nowadays, biosensors are used in diagnostics, food industry, and drug discovery. Biosensors are mainly composed of biomolecules that are coated to the electrode, transducer, and processor. Biomolecules differ depending on the analyte. Some of the examples of biomolecules are enzymes, cells, microorganisms, antibodies, and tissues. The type of transducer can be electrochemical, optical, thermal or acoustic depending on the physicochemical signal analyte produces. (Ramesh et al., 2022; Cho et al., 2020; Mehrotra, 2016; Kheyreddini Mousavi et al., 2012).

Biosensors provide a number of benefits like reliability, biocompatibility, simplicity, and rapid detection. Even though there are many advantages some challenges present in biosensors. Beside the high cost of biosensors, biomolecules that are used are sensitive. Sensitivity of biological molecules affects the stability of biosensor negatively and shortens the lifetime of biosensor. That is why electrochemical sensor is generated in present experiment (Otero & Magner, 2020).

2.5 Working principles of electrochemical sensors

Electrochemical sensors have two different setups: two-electrode system, three-and electrode system. The two-electrode system is composed of working electrode and counter electrode. The three-electrode system is composed of working electrode, counter electrode, and reference electrode. In the present experiment three-electrode system is used (Harris et al., 2023; Fatima et al., 2022).

Maintenance of the potential is kept constant by the reference electrode. The reference electrode in the present experiment was aqueous silver chloride electrode. Saturated calomel electrode (SCE) could be used as a reference electrode. However, Ag/AgCl reference electrode was preferred because it was environment friendly rather than the SCE which contains mercury (Hg). The Ag/AgCl electrode was composed of a silver wire that was coated with silver chloride. The body of the electrode was composed of a plastic tube and contained KCl solution for stabilization. Proportionally to the chloride concentration in the solution, the reference electrode created a potential. The dimensions of the reference electrode were 112x6 mm (Ag/AgCl Reference Electrode | Silver Silver Chloride, n.d.).

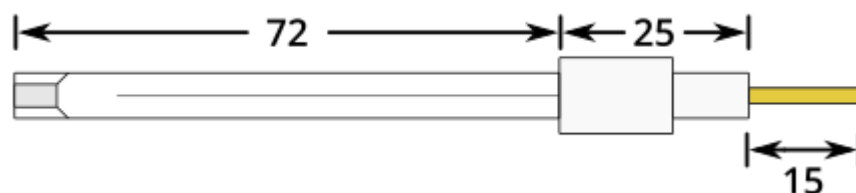


Figure 8: Reference electrode (Ag/AgCl Reference Electrode | Silver Silver Chloride, n.d.)

The oxidation reaction occurs in the counter electrode and balances the reaction. The counter electrode in the present experiment was platinum wire electrode. Gold or carbon can be used instead of platinum. In the two-electrode system, counter electrode act like both counter and reference electrode. In the present experiment, platinum was selected due to its inertness and cheapness over gold. The dimensions of the counter electrode were 82x0.5 mm (Jerkiewicz, 2022; Counter Electrode | Low Price Auxiliary Electrode, n.d.).

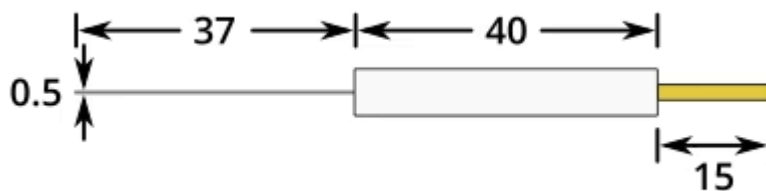


Figure 9: Counter electrode (Counter Electrode | Low Price Auxiliary Electrode, n.d.)

The reduction occurs in the working electrode. The sample of interest is coated to the working electrode. In the present experiment, platinum disc working electrode was used. The dimensions of the working electrode were 100.5x6.15 mm (Platinum Disc Working Electrode | 99.99% Purity, n.d.).

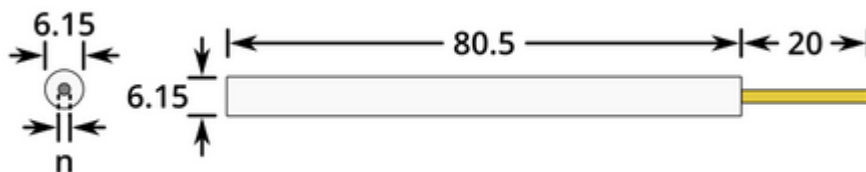


Figure 10: Working electrode (Platinum Disc Working Electrode | 99.99% Purity, n.d.)

2.6 Electrochemical Sensors for Dopamine Detection

In recent years, Dopamine electrochemical sensors have gained a great interest in the research field. Some of the dopamine sensors in the literature are listed below.

Anuar et al. produced hybrid dopamine sensor in 2020. They used platinum and silver metals in addition to the graphene quantum dots to improve the electrocatalytic

activity. Platinum was selected because of its inertness and wide usage in electrochemical sensors applications. Although platinum is a very good metal to produce a sensor, it is very expensive (Anuar et al., 2020).

To minimize platinum use and cost there are two methods. The first one is to couple another metal (i.e., silver) with platinum to minimize the usage. In this experiment, biocompatibility, cost, stability, and abundance made silver a good metal example for the introduction to platinum. The second method to minimize platinum usage is supportive material selection. In this experiment, its high surface area, stability (both thermal and chemical), cost, and conductivity made graphene a good support metal (Anuar et al., 2020).

The aim of this experiment was to check the enhancement in the electrocatalytic activity in graphene supported bimetallic (Pt-Ag) electrochemical sensor. Graphene oxide was synthesized from graphite by Hummers' method. Synthesis of hybrid material was done by mixing $\text{AgNO}_{3(\text{aq})}$, and $\text{K}_2\text{PtCl}_{4(\text{aq})}$ with suspension of graphene. Nafion added hybrid sample was coated to the GCE electrode. Silver-graphene hybrid material, graphene quantum dots, and platinum-graphene hybrid material were synthesized as well for comparison. Field emission scanning electron microscopy (FESEM), Fourier transformed infrared spectroscopy (FTIR), transmission electron microscopy (TEM), X-ray photoelectron spectroscopy (XPS), and EDAX TEAM energy dispersive X-ray (EDX) analysis were done for characterization. CV, EIS, and DPV were performed in a three-electrode system. Platinum counter electrode and SCE reference electrode were used in the system. Influence of scan rates and pH were

checked in the presence of 25 μM dopamine solution. Dopamine hydrochloride injection was used for real sample studies (Anuar et al., 2020).

Results of the experiment was synergetic with the aim. The current of the oxidation peak of dopamine was increased noticeably. The formed hybrid GCE had low limit of detection with 91.4% to 99.0% recovery with dopamine hydrochloride injection (Anuar et al., 2020).

Sabrina Chelly et al. produced gold nanoparticle dopamine sensor in 2021. The standard metal nanoparticle synthesis procedure is complex and expensive. In this experiment like the present experiment, plant extract was used to synthesize metal nanoparticles. Gold is another common metal in electrochemical sensors due to its stability, biocompatibility, and large surface-to-volume ratio. Gold nanoparticles (AuNPs) were synthesized from *Rhanterium suaveolens* (a plant with yellow flower). High amounts of p-coumaric acid and ferulic acid in *Rhanterium suaveolens* plant have roles as stabilizing and reducing agents during gold nanoparticle synthesis. AuNPs were synthesized by adding plant extract to the HAuCl_4 . Scanning electron microscopy (SEM), FESEM, and TEM analysis were done for characterization. Linear Sweep Voltammetry (LSV), and CV at a scan rate of 50 mV/s were performed in the absence and presence of riboflavin and 50 μM dopamine. Cyclic voltammetry results were clearly showed the formation of oxidation peak in the presence of dopamine. Also, the accuracy measurements in different days were proved the stability of modified AuNPs for dopamine detection (Sabrina Chelly et al., 2021).

Huang et al. produced hybrid dopamine sensor in 2021 with nickel metal and metal-organic frameworks. Metal-organic frameworks have large surface area, porous, and diverse but poor conductor for electrochemical sensing. To increase the conductivity of metal-organic frameworks, nickel addition was pursued in this experiment. Ionothermal technique was used to synthesize hybrid material. 5 μ L of Nafion was added to the sample before electrode coating. Thermogravimetric analysis (TGA), SEM, attenuated total reflection Fourier transform infrared spectroscopy (ATR-FTIR), and X-ray diffraction (XRD) analysis were done for characterization. DPV were performed in three-electrode system. Platinum counter electrode and SCE reference electrode were used in the system. The bare electrode gave no response to the presence of dopamine. Dopamine hydrochloride injection was used for real sample studies. However, Ni-MOF electrode gave a huge response compared to the bare electrode in the dopamine presence. The results were accurate in real sample studies as well (Huang et al., 2021).

Huang et al. produced hybrid dopamine sensor in 2020. Multiwalled carbon nanotubes and graphene quantum dots were chosen to form dopamine sensors. Multiwalled carbon nanotubes were used to avoid the distribution of ascorbic acid and uric acid which have similar oxidation potentials and interfere with dopamine and exist in organisms together with dopamine. The aim of the experiment was to ease electron transfer of dopamine by formation of π bonds between graphene quantum dots and multiwalled carbon nanotubes. TEM analysis was done for characterization. CV of bare and coated electrodes were performed in the presence of 0.1 mM dopamine. Anodic peak current of modified electrode was 3.5 times higher than the bare

electrode. Results were showed that the anionic groups in graphene quantum dots combined with multiwalled carbon nanotubes were successful the attract dopamine and not uric acid or ascorbic acid. Limit of detection was low. Real sample studies were done with human serum and living PC12 cells (cells that have a role in dopamine and noradrenaline storage, synthesis, and release). Human serum was undergone 50-fold dilution. Different concentrations of dopamine were added to the serum and DPV was performed. The results were accurate and had low relative standard deviation. Cultured PC12 cells were stimulated with potassium ion to release dopamine. The cells were cultured with hybrid sensor. The good activity of PC12 cells proved the biocompatibility of the hybrid sensor. DPV were performed and successful results were achieved. This experiment was to first experiment that used live PC12 cells in electrochemical sensing of dopamine. (Huang et al., 2020)

Zhang and Liu developed a new approach to graphene quantum dots dopamine sensors in 2020. As mentioned above, graphene is a very good material while forming an electrochemical sensor. Even though there are several advantages, the performance of pure graphene is low. To overcome this problem that limits the applications, heteroatoms like nitrogen, boron, phosphorus, and sulfur were introduced (doped) to pure graphene. Nitrogen doped graphene materials have developed higher performance in electrochemical sensing. In this experiment nitrogen doped graphene were synthesized by the pyrolysis of poly(p-phenylenediamine) rather than the conventional methods to increase nitrogen content and relatively the final yield. DPV and CV were performed in the presence of 0.5 mM dopamine solution. Results have

showed a noticeable change in the presence of dopamine in addition to ascorbic acid and uric acid (Zhang and Liu, 2020).

Gaidukevic et al. produced graphene-based dopamine sensors in 2022. Like Zhang and Liu, Gaidukevic et al were decided to modify graphene materials. Graphene oxide was reduced by conventional Hummers' method and modified Hummers' method. In modified Hummers' method pristine graphite powder was pre-oxidized by the mixture of H_2SO_4 , CrO_3 , H_3BO_3 . Raman spectroscopy, XPS and SEM analysis were done for characterization. CV and DPV were performed in the presence and absence of $50 \mu\text{M}$ dopamine. The higher sensibility was obtained from sensor that has made by modified Hummers' method (Gaidukevic et al., 2022).

Yang et al. developed hybrid dopamine sensor 2022. The materials for the hybrid sensor formation were carbon nanotubes and cementite. Reaction in the carbon layer and ferrocene pyrolysis caused iron carbide attachment to carbon nanotubes. High-resolution transmission electron microscopy (HRTEM), XRD, XPS, SEM analysis were done for characterization. CV, and DPV were performed in a three-electrode system. Platinum counter electrode and Ag/AgCl reference electrode were used in the system. The peak current of dopamine was increased proportionally by concentration addition. Uric acid showed two times lower peaks than dopamine which indicates that carbon nanotubes-cementite sensor is more sensitive to dopamine. Non-toxicity, low synthesise time, and increased electrochemical conductivity are the advantages of this hybrid sensor (Yang et al., 2022).

Li et al. developed hybrid dopamine sensor for human serum in 2021. Non-toxicity, high reaction rate, stability, and biocompatibility made nanostructured metal oxides a good material in electrochemical sensing. Copper oxide nanoparticles were chosen due to their adhesion and absorption capacities. Silver nanoparticles were hybridized with CuO nanoparticles to increase electron transportation. EDX and TEM analysis were done for characterization. CV, and DPV were performed in the presence of 50 μ M dopamine. The serum sample results with a recovery range 95.7% to 111.1% have proved the reliability of this sensor (Li et al., 2021).

Yao Shen Chen et al. developed a dopamine sensor in 2019. In this experiment heteroatom doping to the graphene material were done. Like Zhang and Liu, nitrogen was chosen for doping. N-doped graphitic carbon sheets formed hybrid structure with iron carbide. SEM, TEM, and XRD analysis were done for characterization. EIS and CV were performed in the presence of dopamine. However, limit of detection range was high in this experiment (Yao Shen Chen et al., 2019).

Lastly, Feng et al. developed a hybrid dopamine sensor in 2022. Covalent organic frameworks have good stability (both chemical and thermal), and high surface area but poor conductivity. In this experiment, researchers aimed to increase the conductivity of covalent organic frameworks by introduction of platinum and carboxylated multi-walled carbon nanotubes. TEM, SEM, XRD, and EDX analysis were done for characterization. EIS and CV were performed in the presence of 0.5 mM dopamine. As a result, the purpose of the experiment was achieved, reliable sensitive dopamine sensor was developed (Feng et al., 2022).

Chapter 3

EXPERIMENTAL STUDY

3.1 Reagents and Materials

Orange peels, *Bougainvillea* leaves, HCl (37%), Ni(NO₃)₂·6H₂O which has a molar mass of 290.8 g/mol, 0.05 micron Alumina polish, ethanol, Nafion, Ag/AgCl reference electrode, Platinum counter electrode, Glassy carbon working electrode, NaCl, Na₂HPO₄ which has a molar mass of 141.97 g/mol, NaH₂PO₄·2H₂O which has a molar mass of 156.01 g/mol, KCl, Na₂SO₄ which has a molar mass of 142.04 g/mol, dopamine which has a molar mass of 189.64 g/mol, urea which has a molar mass of 60.06 g/mol, ascorbic acid which has a molar mass of 176.12 g/mol, uric acid which has a molar mass of 168.11 g/mol, glucose monohydrate which has a molar mass of 198.17 g/mol, fructose which has a molar mass of 180.16 g/mol, citric acid which has a molar mass of 210.15 g/mol urine obtained from healthy human, blood obtained from healthy human, and serum obtained from healthy human, were used in this experiment.

3.2 Experimental

3.2.1 Synthesis of Graphene Quantum Dots

Orange peels were collected. Orange peels dried in the oven for a week in 100 °C. Dried orange peels were turned into powder by crushing. A solution containing 0.75 g of powdered orange peel with 50 mL of distilled water was prepared. Solution was stirred for 30 minutes at room temperature. The solution was transferred into Teflon-lined

autoclave. The autoclave was heated in furnace for 6 hours in 180 °C. Distilled water was added to the final product and the final product was centrifuged for 20 minutes at 3000 rpm. The supernatant of the centrifuged product was collected. Liquid quantum dots were stored in the fridge at 4°C.

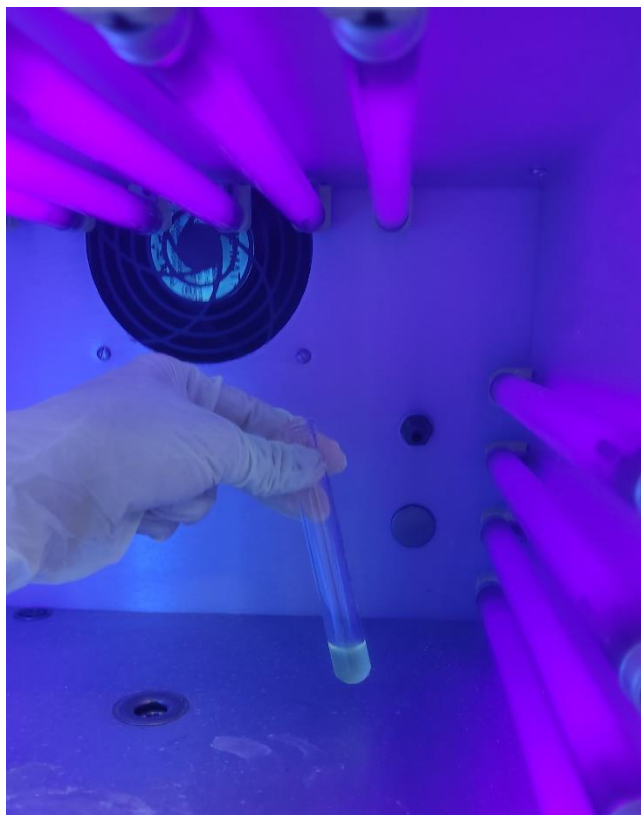


Figure 11: Graphene Quantum Dots under UV light.

3.2.2 Synthesis of NiO Nanoparticles

Fresh *Bougainvillea* leaves were collected. The *Bougainvillea* leaves were washed with distilled water and dried in drying machine for 6 hours. Dried leaves were ground and were sieved using 15-mesh sieve. 2% of HCl was added into the leave powder. The

solution was filtered and dried in micro-oven for 6 hours at 50 °C. 2.0 g of HCl treated leave powder was added to 100 mL of distilled water. The solution was stirred for 2 hours in room temperature. Then, stirred solution was sonicated for 1 hour. The precipitate was removed by filtration. The plant extract was collected.

80 mL of 0.1 M $\text{Ni}(\text{NO}_3)_2 \cdot 6\text{H}_2\text{O}$ solution was prepared. The $\text{Ni}(\text{NO}_3)_2 \cdot 6\text{H}_2\text{O}$ solution was transferred to the stirrer. The $\text{Ni}(\text{NO}_3)_2 \cdot 6\text{H}_2\text{O}$ was stirred at 90°C for 3 hours. While the $\text{Ni}(\text{NO}_3)_2 \cdot 6\text{H}_2\text{O}$ solution was stirring, 80 mL of plant extract was added dropwise. The solution was freeze-dried in 8 hours shifts for 3 days. Freeze-dried paste-textured nanoparticles were collected.

Due to the problem in the freeze-dried machine, half of the nanoparticles were obtained by combustion method. The solution was heated in the micro-oven instead of freeze-dried machine for 12 hours. Then, it was transferred to the porcelain crucibles. The material was heated in the furnace for 3 hours at 400°C. The end product was collected.

3.2.3 Synthesis of Hybrid Quantum Dots

0.5 g of powdered orange peel was added to 50 mL of distilled water. 0.25 g of NiO nanoparticles were added to the solution. The solution was stirred for 20 minutes at room temperature. Then the solution was transferred into sonicator and was sonicated for 20 minutes. The solution was transferred into Teflon-lined autoclave. The autoclave was heated in furnace for 6 hours in 180 °C. Distilled water was added to the final product and the final product was centrifuged for 20 minutes at 3000 rpm. The precipitate of the centrifuged product was collected. The end product was named as “1-Hybrid.”

Same procedure was applied in the preparation of two other hybrids. Hybrid called “2-Hybrid” contains 0.5 g of powdered orange peel and 0.5 g of NiO nanoparticles. Hybrid called “3-Hybrid” contains 0.25 g of powdered orange peel and 0.5 g of NiO nanoparticles.

3.2.4 Characterization

The synthesized materials were examined using a Fournier Transform Infrared Spectrophotometer (FTIR). The samples were sent to the Turkey for SEM, XPS, XRD, and BET analysis.

3.2.5 Preparation of Ferrocyanide and Sodium Sulphate Stock Solutions

0.1 M 200 mL of KCl solution was prepared by mixing 1.5 g of KCl with 200 mL of distilled water. 0.066 g $K_3[Fe(CN)_6]$ was weighed and mixed with 200 mL of KCl solution to form ferrocyanide ion ($[Fe(CN)_6]^{4-}$). The 1 mM ferrocyanide solution was prepared for electrochemical analysis.

Sodium sulphate solution was prepared by adding 2.8408 g of sodium sulphate (Na_2SO_4) to 200 mL distilled water. The sodium sulphate solution was prepared for electrochemical analysis.

3.2.6 Modified Electrode Fabrication and Preparation

2 mg NiO nanoparticles were weighed and were mixed with 1 mL of distilled water in the Eppendorf tube. The tube was sonicated for 10 minutes. 2 drops of Nafion and 2 drops of ethanol were added to the solution. Then, the tube was sonicated for 10 minutes. Same procedure was applied for three different hybrid quantum dots. Since the graphene

quantum dots were liquid, 1 mL of quantum dots was added to the Eppendorf tube instead of distilled water.

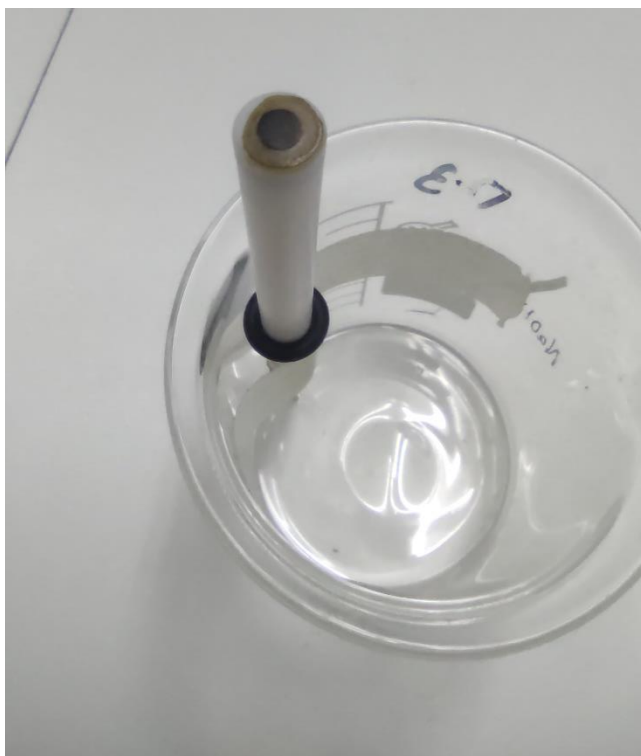


Figure 12: Coated electrode

Glassy carbon bare working electrode was polished with 0.05-micron Alumina polish. The electrode was rinsed with distilled water. 20 μL of nafion-mixed quantum dots were added to the electrode for coating by micropipette. The electrode was dried under infrared lamp for 30 minutes. After completely drying of the quantum dots, again 20 μL of nafion-mixed quantum dots were added for second coating. The electrode was dried under infrared lamp for another 30 minutes. The coated electrode was prepared.

3.2.7 Preparation of Phosphate-buffered Saline Solution

Phosphate-buffered Saline (PBS) was used as a buffer for pH level maintenance. 0.1 M 7.0 pH PBS was prepared by adding 8 g of NaCl, 0.2 g of KCl, 1.44g of Na₂HPO₄, and 0.28 g of NaH₂PO₄·2H₂O instead of potassium phosphate monobasic to 1L distilled water.

3.2.8 Preparation of Dopamine Solutions

The 100 mL stock solution which has a concentration of 500 μM was prepared by adding 0.09482 g of dopamine (chemical name) which has a molar mass of g/mol to PBS solution. Then, solutions which have different concentrations (400 μM, 300 μM, 200 μM, 100 μM, 50 μM, 25 μM, 10 μM, 5 μM, 3.5 μM, 2.5 μM, 1.5 μM, 1.0 μM, 0.5 μM, 0.2 μM, 0.1 μM, 0.05 μM, 0.01 μM, 0.005 μM, 0.001 μM) were prepared by serial dilution method.

3.2.9 Preparation of Real Samples

In this research, blood, blood serum and urine were used for real sample studies. Samples were collected.

Urine sample was centrifuged for 20 minutes at 3000 rpm. The centrifuged urine sample was filtered to remove precipitated proteins and other particulate matters. The urine sample was diluted 50-fold with PBS. 50 μL of whole blood was diluted to 100 μL with PBS buffer. Lastly, the blood serum was diluted 10-fold with PBS.

3.3 Electrochemical Test

Three electrode system was established. The three-electrode system was equipped with bare (working) electrode, Ag/AgCl reference electrode, and platinum wire counter electrode. The potentiostat that has been used for supply is called “Sensit Smart Smart

Phone Potentiostat” from PalmSens company. The following picture shows the setup of a three-electrode system.



Figure 13: Three-electrode system with ferrocyanide

First of all, bare electrode, and coated electrode with all materials (QDs, nanoparticles, 1-Hybrid, 2-Hybrid, and 3-Hybrid) were run cyclic voltammetry (CV) separately in 1mM Ferrocyanide at different scan rates. The scan rates were: 10 mV/s , 20 mV/s, 30 mV/s, 40 mV/s, 50 mV/s, 75 mV/s, 100 mV/s, 150 mV/s, and 200 mV/s respectively. Electroactive surface area of all materials (QDs, nanoparticles, 1-Hybrid, 2-Hybrid, and 3-Hybrid) were calculated.

Next, electrochemical impedance spectroscopy (EIS) of all materials and bare electrode were run in 1mM Ferrocyanide separately. In addition to the Ferrocyanide, all materials (QDs, nanoparticles, 1-Hybrid, 2-Hybrid, and 3-Hybrid) and bare electrode were run EIS separately in 0.1 M sodium sulphate at different for comparison of electrolyte solutions. Ferrocyanide were chosen as a result of accuracy.

2-Hybrid were chosen between three different hybrid samples due to its higher oxidation values. The next steps of the experiment were continued with 2-Hybrid. However, to see the mechanism of all materials, the five samples and bare electrode was run CV at 100 mV/s in PBS buffer before starting dopamine detection. Note that the bare electrode was run CV five times in PBS for limit of detection (LOD) and limit of quantification (LOQ) analyses.

Cyclic voltammetry was run in three electrode system with 2-Hybrid coated working electrode. 2-Hybrid were examined in different dopamine concentrations (500 Mm, 400 μ M, 300 μ M, 200 μ M, 100 μ M, 50 μ M, 25 μ M, 10 μ M, 5 μ M, 3.5 μ M, 2.5 μ M, 1.5 μ M, 1.0 μ M, 0.5 μ M, 0.2 μ M, 0.1 μ M, 0.05 μ M, 0.01 μ M, 0.005 μ M, 0.001 μ M). Calibration curve was prepared using these concentrations' CV results.

Differential pulse voltammetry (DPV) was run in three electrode system with 2-Hybrid coated working electrode. 2-Hybrid were examined in different dopamine concentrations (10 μ M, 5 μ M, 2.5 μ M, 1.5 μ M, 1.0 μ M, 0.5 μ M, 0.2 μ M, and 0.1 μ M).

2.5 μM dopamine solution was used to check the effect of different scan rates in 2-Hybrid coated electrode. The scan rates that has been used are; 10 mV/s, 25 mV/s, 50 mV/s, 75 mV/s, 100 mV/s, and 150 mV/s.

For the repeatability studies, the same 2-Hybrid coated GCE electrode was run CV for 10 times at 100 mV/s in the presence of 2.5 μM dopamine solution. Relative standard deviation (RSD) was calculated.

For the reproducibility studies, five different 2-Hybrid coated GCE electrode was run CV at 100 mV/s in the presence of 2.5 μM dopamine solution. Relative standard deviation (RSD) was calculated.

For the stability studies, first, the same 2-Hybrid coated GCE electrode was run CV for 20 times at 100 mV/s in the presence of 2.5 μM dopamine solution. Relative standard deviation (RSD) was calculated. Second, the same 2-Hybrid coated GCE electrode was run CV for 5 times in the presence of 2.5 μM dopamine solution. After each electrochemical measurement, the electrode was rinsed with distilled water and was kept in the refrigerator at 4 $^{\circ}\text{C}$ for three days. The second step was lasted for two weeks.

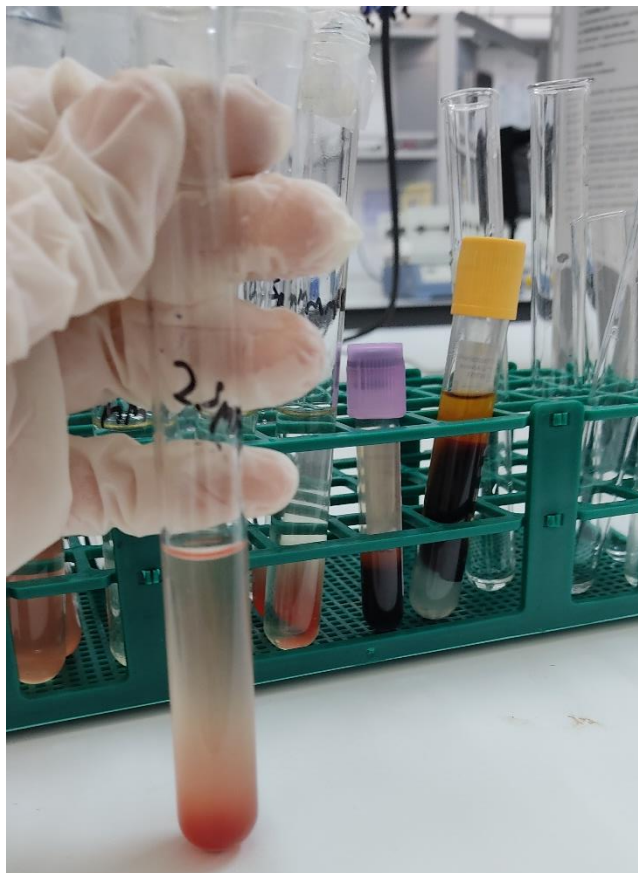


Figure 14: Diluted blood sample

For real sample studies, 50-fold diluted urine was used as electrolyte in cyclic voltammetry at 100 mV/s and differential pulse voltammetry of 2-Hybrid coated GCE electrode. Diluted urine was divided into five different bottles. 1.5 μM , 2.5 μM , 3.5 μM , and 5 μM dopamine solutions were added to different bottles and one bottle was left as control. The peak currents were recorded. To calculate RSD this procedure was repeated three times.

10-fold diluted serum was used as electrolyte in cyclic voltammetry at 100 mV/s and differential pulse voltammetry of 2-Hybrid coated GCE electrode. 10 μM , 5 μM , 2.5 μM ,

1 μM and 0.5 μM dopamine solutions were added to the diluted serum separately. The peak currents were recorded. To calculate RSD this procedure was repeated three times.

Diluted whole human blood was used as electrolyte in cyclic voltammetry at 100 mV/s and differential pulse voltammetry of 2-Hybrid coated GCE electrode. 10 μM , 5 μM , 2.5 μM , 1 μM and 0.5 μM dopamine solutions were added to the diluted blood separately. The peak currents were recorded. To calculate RSD this procedure was repeated three times.

For selectivity or interference studies, first, CV and DPV were performed in the presence of 100 μM uric acid, 100 μM citric acid, 100 μM ascorbic acid, 100 μM dopamine, 100 μM NaCl, 100 μM glucose monohydrate, 100 μM fructose, 100 μM KCl, and mixture of each species respectively. Second, amperometry was carried out with a potential of 0.18 V, 1.0 s of t_{interval} , and 800 s of t_{run} . 0.5 M 5 mL dopamine was prepared. 25 μL of each 100 μM sample and at the end, 50 μL of dopamine were added one by one to achieve 2.5 mM analyte.

Chapter 4

RESULTS AND DISCUSSIONS

4.1 FTIR Analysis Results

Fourier-transform infrared spectroscopy was used for characterization. The FTIR results of three hybrid materials can be seen below.

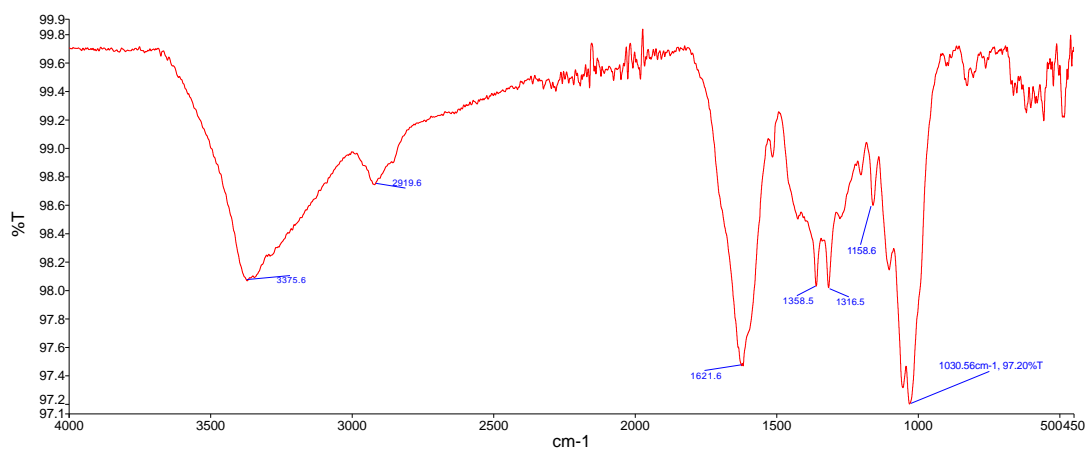


Figure 15: FTIR of 1-hybrid

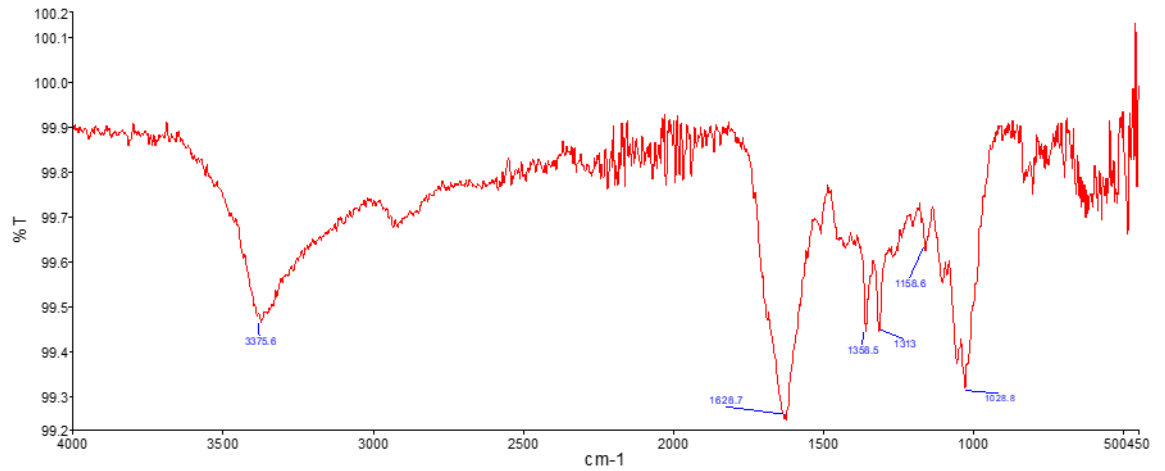


Figure 16: FTIR of 2-hybrid

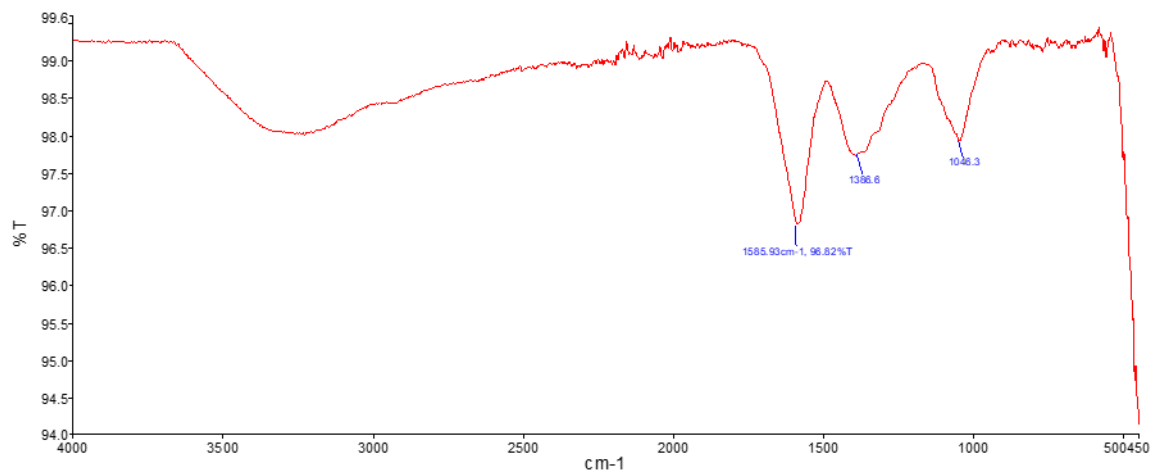


Figure 17: FTIR of 3-hybrid

The broad peaks between 3600-3200 cm⁻¹ represent O-H stretching. The medium intensity peaks appeared between 3300-2700 cm⁻¹ in 1-hybrid and 2-hybrid represent C-H group. The peaks appeared between 1650-1550 cm⁻¹ represent C=N stretching. Peaks between 500-450 cm⁻¹ in 1-hybrid and 2-hybrid represent Ni-O bending.

4.2 Electroactive Surface Area of Materials in Ferrocyanide

Cyclic voltammetry results of hybrid materials can be seen below.

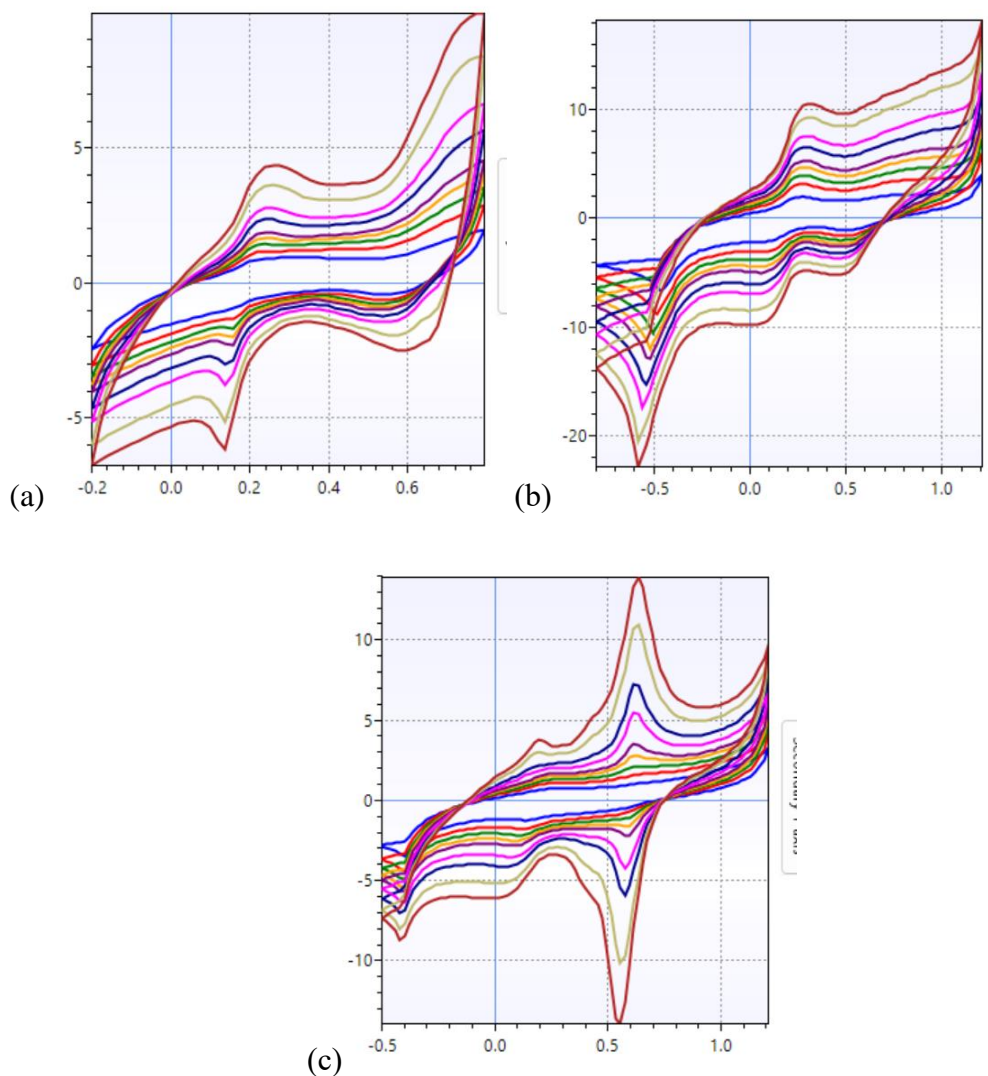


Figure 18: CVs of (a)1-hybrid (b) 2-hybrid (c) 3-hybrid

Cyclic voltammetry of all materials was performed to calculate electroactive surface area.

Randles Sevcik equation was rewrite for calculation.

$$slope = \frac{I_{pc}}{\sqrt{v}} = 2.69 \times 10^8 \times n^{3/2} \times A \times D \times C$$

Where I_{pc} indicates peak current in A, v indicates scan rate in mV/s, n indicates the number of electrons transferred for the redox reaction ($n=1$), A indicates electroactive surface area in m^2 , D indicates diffusion coefficient in m^2/s ($D= 7.6 \times 10^{-12}$), and C indicates concentration in M ($C=10^{-3}$ M). Results are listed in Table 1.

Table 1: Electroactive surface area results

Material	Electroactive Surface Area (m^2)
Bare electrode	4.045×10^{-6}
NiO nanoparticles	2.697×10^{-6}
Graphene Quantum Dots	1.348×10^{-6}
1-hybrid	1.348×10^{-6}
2-hybrid	2.697×10^{-6}
3-hybrid	5.394×10^{-6}

The electroactive surface area of 3-hybrid is higher than the electroactive surface area of bare electrode.

4.3 EIS Results of Materials in Ferrocyanide

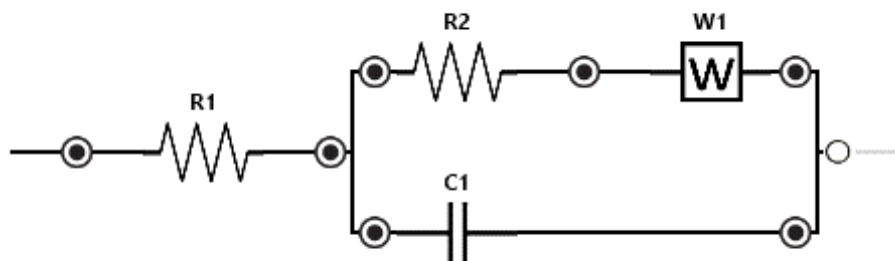


Figure 19: EIS diagram

Table 2: EIS results depending on the diagram above.

Material	R1 (Ω)	R2 (Ω)	W1 ($k\sigma$)	C1 (nF)
Bare electrode	322	0.304	52.26	1.0×10^4
NiO nanoparticles	164	1.0×10^{-6}	40.80	71.98
Graphene Quantum Dots	171.2	0.178	31.92	1.4×10^4
1-hybrid	218.2	0.015	23.93	1.4×10^4
2-hybrid	165.7	0.016	17.49	1.3×10^4
3-hybrid	188	0.048	2198	8330

4.4 Calibration Curve

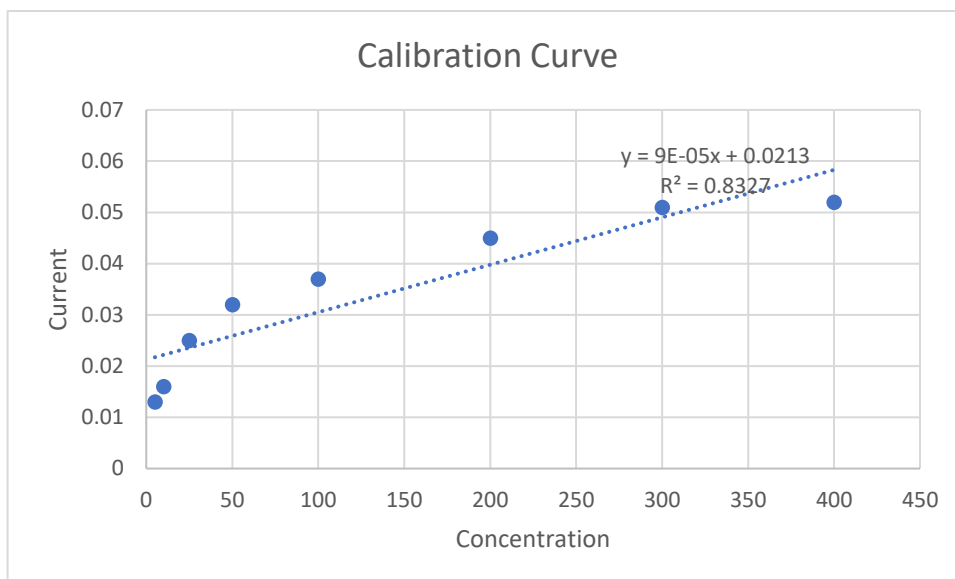


Figure 20: Calibration Curve

Calibration curve is drawn using the CV results of 2-hybrid in different dopamine concentrations.

4.5 Limit of Detection and Limit of Quantification Calculations

Limit of detection and limit of quantification were calculated using the equations below.

$$LOD = \frac{3 \times \sigma \text{ of blank}}{\text{slope of calibration curve}}$$

$$LOQ = \frac{10 \times \sigma \text{ of blank}}{\text{slope of calibration curve}}$$

LOD was calculated 310.7 and LOQ was calculated 1035.6.

4.6 Relative Standard Deviation Calculations

RSD results were calculated using the equation below.

$$RSD \% = \frac{\sigma}{mean} \times 100$$

Table 3: RSD results

	RSD%
Repeatability studies	11.4
Reproducibility studies	11.75
Stability studies	12

Table 4: RSD results of blood sample

	RSD%
10 μM	4.2
5 μM	2.5
2.5 μM	5.0
1 μM	2.75
0.5 μM	4.2

Table 5: RSD results of serum sample

	RSD%
10 μM	2.16
5 μM	5.1
2.5 μM	2.8
1 μM	5.23
0.5 μM	3.2

Table 6: RSD results of urine sample

	RSD%
Control	5.67
1.5 μM	4.76
2.5 μM	0.4
3.5 μM	2.13
5 μM	2.4

4.7 Stability studies

For the second step of stability studies the same 2-Hybrid coated GCE electrode was run CV for 5 times in the presence of 2.5 μM dopamine solution. After each electrochemical measurement, the electrode was rinsed with distilled water and was kept in the refrigerator at 4 $^{\circ}\text{C}$ for three days. The second step lasted for two weeks. Results are shown in figure 18. The results are accurate except for the first reading. A drastic decrease has been noticed between the first and second readings.

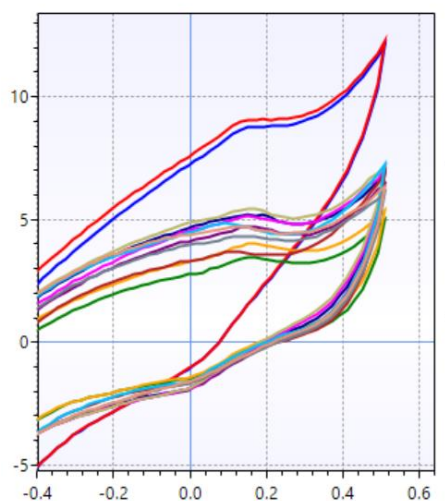


Figure 21: CV results of stability studies

4.8 Results of Selectivity Studies

CV and DPV results of 100 μM uric acid, 100 μM citric acid, 100 μM ascorbic acid, 100 μM dopamine, 100 μM NaCl, 100 μM glucose monohydrate, 100 μM fructose, and 100 μM KCl are shown below.

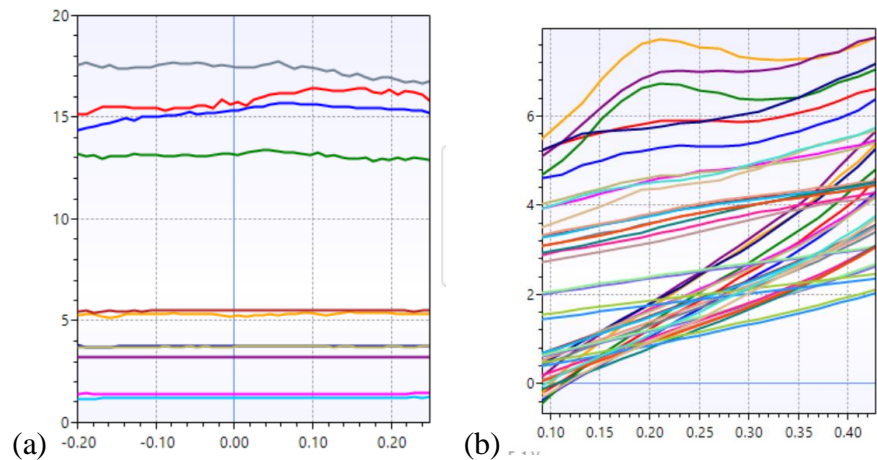


Figure 22: Selectivity results (a)DPV (b)CV

4.9 Amperometry results

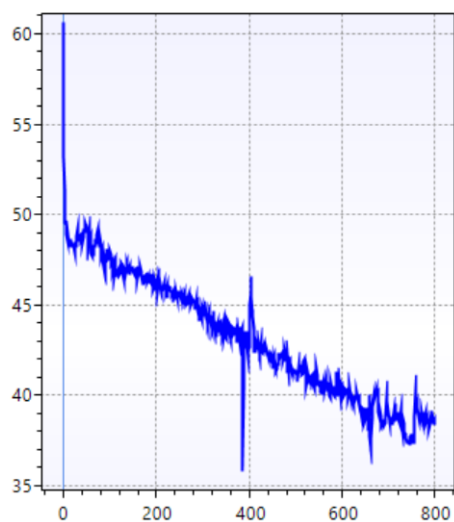


Figure 23: Amperometry results

4.10 Discussion

In the present experiment enhancement of conductivity and sensitivity was expected in hybrid materials. FTIR results clearly show the successful formation of the hybrid structures. 2-hybrid was chosen due to the accuracy between peaks in CV results, low resistance value in EIS results and high correlation coefficient (0.9975). In cyclic

voltammetry, a decrease in peak current is expected while concentration of the analyte decreases. During CV for different dopamine concentrations, readings in nano level showed inaccurate results. Also, the peak for 500 μM dopamine solution was less than the peak of 400 μM . It can be said that the hybrid sensor can detect dopamine in micro level up to 500 μM .

The oxidation peaks of real samples were proportionally increased with concentration change. Relative standard deviation percentages are low which indicates the precision of the sensor.

The CV results of the selectivity studies were hopeful. The highest peak was detected in dopamine presence. Uric acid has the highest peak among the materials except PBS, and dopamine. The peak of uric acid was 1.4 times lower than the peak of dopamine. In addition, lowest peaks belonged to fructose, and urea.

In amperometry, addition of only dopamine, uric acid and citric acid caused a change in current. The stability of sensor was accurate in two weeks except the first reading.

Chapter 5

CONCLUSION

In this study, electrochemical dopamine sensing from NiO-graphene quantum dots hybrid material was carried out. The materials were characterized using FTIR. Below are the summarized results:

- The oxidation and reduction peaks of all materials were increased proportionally with the scan rate in ferrocyanide.
- The oxidation peak of developed sensor was increased proportionally with the dopamine concentration up to 500 μM .
- The sensor was able to detect dopamine in urine, blood, and serum samples. The CV peaks were increased proportionally with the concentration.
- The sensor interacts with uric acid more than other materials. However, dopamine still has the highest peak.

In conclusion, the purpose of the experiment was accomplished. The conductivity and sensitivity were enhanced using hybrid sensor. The developed sensor is stable and detects dopamine correctly.

REFERENCES

- Alhadj, M., & Farhana, A. (2020, February 2). Enzyme Linked Immunosorbent Assay (ELISA). PubMed; StatPearls Publishing. <https://www.ncbi.nlm.nih.gov/books/NBK555922/>
- An, J. H., Choi, D.-K., Lee, K.-J., & Choi, J.-W. (2015). Surface-enhanced Raman spectroscopy detection of dopamine by DNA Targeting amplification assay in Parkinsons's model. *Biosensors and Bioelectronics*, 67, 739–746. <https://doi.org/10.1016/j.bios.2014.10.049>
- Anagu, L. O., & Andoh, N. E. (2022, January 1). Chapter 4 - Vaccine development: from the laboratory to the field (R. Ashfield, A. N. Oli, C. Esimone, & L. Anagu, Eds.). ScienceDirect; Academic Press. <https://www.sciencedirect.com/science/article/abs/pii/B9780323911467000111>
- Anuar, N. S., Basirun, W. J., Shalauddin, Md., & Akhter, S. (2020). A dopamine electrochemical sensor based on a platinum–silver graphene nanocomposite modified electrode. *RSC Advances*, 10(29), 17336–17344. [https://doi.org/10.1039/c9ra11056aAg/AgCl Reference Electrode | Silver Silver Chloride. \(n.d.\). Ossila. https://www.ossila.com/en-eu/products/ag-agcl-reference-electrode](https://doi.org/10.1039/c9ra11056aAg/AgCl Reference Electrode | Silver Silver Chloride. (n.d.). Ossila. https://www.ossila.com/en-eu/products/ag-agcl-reference-electrode)

- Arumugasamy, S. K., Govindaraju, S., & Yun, K. (2020). Electrochemical sensor for detecting dopamine using graphene quantum dots incorporated with multiwall carbon nanotubes. *Applied Surface Science*, 508, 145294. <https://doi.org/10.1016/j.apsusc.2020.145294>
- Aydin, B. S., & Bulduk, İ. (2020). A Validated HPLC-UV Method for Determination of Dopamine HCl in Injectable Solutions. *Eurasian Journal of Biological and Chemical Sciences*, 3(2), 116–120. <https://dergipark.org.tr/en/pub/ejbcs/issue/58643/822937>
- Berends, Eisenhofer, Fishbein, Horst-Schriever, Kema, Links, Lenders, & Kerstens. (2019). Intricacies of the Molecular Machinery of Catecholamine Biosynthesis and Secretion by Chromaffin Cells of the Normal Adrenal Medulla and in Pheochromocytoma and Paraganglioma. *Cancers*, 11(8), 1121. <https://doi.org/10.3390/cancers11081121>
- Chatterjee, M., Nath, P., Kadian, S., Kumar, A., Kumar, V., Roy, P., Manik, G., & Satapathi, S. (2022). Highly sensitive and selective detection of dopamine with boron and sulfur co-doped graphene quantum dots. *Scientific Reports*, 12(1). <https://doi.org/10.1038/s41598-022-13016-4>
- Cho, I.-H., Kim, D. H., & Park, S. (2020). Electrochemical biosensors: perspective on functional nanomaterials for on-site analysis. *Biomaterials Research*, 24(1). <https://doi.org/10.1186/s40824-019-0181-y>

Cinquanta, L., Fontana, D. E., & Bizzaro, N. (2017). Chemiluminescent immunoassay technology: What does it change in autoantibody detection? *Autoimmunity Highlights*, 8(1). <https://doi.org/10.1007/s13317-017-0097-2>

Counter Electrode | Low Price Auxiliary Electrode. (n.d.). Ossila. Retrieved June 17, 2023, from <https://www.ossila.com/en-eu/products/counter-electrode>

Fang, H., Pajski, M. L., Ross, A. E., & Venton, B. J. (2013). Quantitation of dopamine, serotonin and adenosine content in a tissue punch from a brain slice using capillary electrophoresis with fast-scan cyclic voltammetry detection. *Analytical Methods*, 5(11), 2704. <https://doi.org/10.1039/c3ay40222c>

Fatima, T., Bansal, S., Husain, S., & Khanuja, M. (2022, January 1). 1 - Biosensors (G. Maruccio & J. Narang, Eds.). ScienceDirect; Woodhead Publishing. <https://www.sciencedirect.com/science/article/abs/pii/B9780128231487000015>

Feng, S., Yan, M., Xue, Y., Huang, J., & Yang, X. (2022). An electrochemical sensor for sensitive detection of dopamine based on a COF/Pt/MWCNT–COOH nanocomposite. *Chemical Communications*, 58(41), 6092–6095. <https://doi.org/10.1039/D2CC01376B>

Fernandez-Chiappe, F., Hermann-Luibl, C., Peteranderl, A., Reinhard, N., Senthilan, P. R., Hieke, M., Selcho, M., Yoshii, T., Shafer, O. T., Muraro, N. I., & Helfrich-Förster, C. (2020). Dopamine Signaling in Wake-Promoting Clock Neurons Is Not Required

for the Normal Regulation of Sleep in *Drosophila*. *The Journal of Neuroscience*, 40(50), 9617–9633. <https://doi.org/10.1523/jneurosci.1488-20.2020>

Ferry, B., Gifu, E.-P., Sandu, I., Denoroy, L., & Parrot, S. (2014). Analysis of microdialysate monoamines, including noradrenaline, dopamine and serotonin, using capillary ultra-high performance liquid chromatography and electrochemical detection. *Journal of Chromatography B*, 951-952, 52–57. <https://doi.org/10.1016/j.jchromb.2014.01.023>

Franco, R., Reyes-Resina, I., & Navarro, G. (2021). Dopamine in Health and Disease: Much More Than a Neurotransmitter. *Biomedicines*, 9(2), 109. <https://doi.org/10.3390/biomedicines9020109>

Gaidukevic, J., Aukstakojyte, R., Barkauskas, J., Niaura, G., Murauskas, T., & Pauliukaite, R. (2022). A novel electrochemical sensor based on thermally reduced graphene oxide for the sensitive determination of dopamine. *Applied Surface Science*, 592, 153257. <https://doi.org/10.1016/j.apsusc.2022.153257>

Harris, A. R., Grayden, D. B., & John, S. E. (2023). Electrochemistry in a Two- or Three-Electrode Configuration to Understand Monopolar or Bipolar Configurations of Platinum Bionic Implants. 14(4), 722–722. <https://doi.org/10.3390/mi14040722>

Horlock, C. (n.d.). Enzyme-linked immunosorbent assay (ELISA) | British Society for Immunology. www.immunology.org. <https://www.immunology.org/public->

information/bitesized-immunology/experimental-techniques/enzyme-linked-immunosorbent-assay#:~:text=The%20enzyme%2Dlinked%20immunosorbent%20assay

Huang, Q., Lin, X., Tong, L., & Tong, Q.-X. (2020). Graphene Quantum Dots/Multiwalled Carbon Nanotubes Composite-Based Electrochemical Sensor for Detecting Dopamine Release from Living Cells. *8*(3), 1644–1650. <https://doi.org/10.1021/acssuschemeng.9b06623>

Huang, Z., Zhang, L., Cao, P., Wang, N., & Lin, M. (2021). Electrochemical sensing of dopamine using a Ni-based metal-organic framework modified electrode. *Ionics*, *27*(3), 1339–1345. <https://doi.org/10.1007/s11581-020-03857-2>

Jerkiewicz, G. (2022). Applicability of Platinum as a Counter-Electrode Material in Electrocatalysis Research. *ACS Catalysis*, *12*(4), 2661–2670. <https://doi.org/10.1021/acscatal.1c06040>

Kim, J., Jeon, M., Paeng, K.-J., & Paeng, I. R. (2008). Competitive enzyme-linked immunosorbent assay for the determination of catecholamine, dopamine in serum. *Analytica Chimica Acta*, *619*(1), 87–93. <https://doi.org/10.1016/j.aca.2008.02.042>

Klein, M.O., Battagello, D.S., Cardoso, A.R., Hauser, D.N., Bittencourt, J.C. and Correa, R.G. (2018). Dopamine: Functions, Signaling, and Association with Neurological

Diseases. Cellular and Molecular Neurobiology, 39(1), pp.31–59.
doi:<https://doi.org/10.1007/s10571-018-0632-3>.

Lakard, S., Pavel, I.-A., & Lakard, B. (2021). Electrochemical Biosensing of Dopamine Neurotransmitter: A Review. Biosensors, 11(6), 179.
<https://doi.org/10.3390/bios11060179>

Lan, Y., Yuan, F., Tadesse Haile Fereja, Wang, C., Lou, B., Li, J., & Xu, G. (2019). Chemiluminescence of Lucigenin/Riboflavin and Its Application for Selective and Sensitive Dopamine Detection. 91(3), 2135–2139.
<https://doi.org/10.1021/acs.analchem.8b04670>

Li, Y.-Y., Kang, P., Wang, S.-Q., Liu, Z.-G., Li, Y.-X., & Guo, Z. (2021). Ag nanoparticles anchored onto porous CuO nanobelts for the ultrasensitive electrochemical detection of dopamine in human serum. Sensors and Actuators B: Chemical, 327, 128878. <https://doi.org/10.1016/j.snb.2020.128878>

Lozano-Sánchez, J., Borrás-Linares, I., Sass-Kiss, A., & Segura-Carretero, A. (2018, January 1). Chapter 13 - Chromatographic Technique: High-Performance Liquid Chromatography (HPLC) (D.-W. Sun, Ed.). ScienceDirect; Academic Press.
<https://www.sciencedirect.com/science/article/abs/pii/B978012814264600013X>

Mehrotra, P. (2016). Biosensors and their applications – A review. Journal of Oral Biology and Craniofacial Research, 6(2), 153–159. <https://doi.org/10.1016/j.jobcr.2015.12.002>

Nichkova, M., Wynveen, P. M., Marc, D. T., Huisman, H., & Kellermann, G. H. (2013).

Validation of an ELISA for urinary dopamine: applications in monitoring treatment of dopamine-related disorders. *Journal of Neurochemistry*, 125(5), 724–735.

<https://doi.org/10.1111/jnc.12248>

Otero, F., & Magner, E. (2020). Biosensors—Recent Advances and Future Challenges in

Electrode Materials. *Sensors*, 20(12), 3561. <https://doi.org/10.3390/s20123561>

Petrova, O. E., & Sauer, K. (2017). High-Performance Liquid Chromatography (HPLC)-

Based Detection and Quantitation of Cellular c-di-GMP. *C-Di-GMP Signaling*, 1657, 33–43. https://doi.org/10.1007/978-1-4939-7240-1_4

PubChem. (n.d.). Dopamine. [Pubchem.ncbi.nlm.nih.gov](https://pubchem.ncbi.nlm.nih.gov). Retrieved June 14, 2023, from

<https://pubchem.ncbi.nlm.nih.gov/compound/Dopamine#section=13C-NMR-Spectra>

Sabrine Chelly, Meryam Chelly, Rayhane Zribi, Radhouane Gdoura, Hanen Bouaziz-

Ketata, & Neri, G. (2021). Electrochemical Detection of Dopamine and Riboflavine on a Screen-Printed Carbon Electrode Modified by AuNPs Derived from *Rhanterium suaveolens* Plant Extract. *6(37)*, 23666–23675.

<https://doi.org/10.1021/acsomega.1c00793>

Sethu, S., Sharma, N., Acharya, S., Nair, A., Matalia, J., Shetty, R., & Ghosh, A. (2019).

Dopamine levels in human tear fluid. *Indian Journal of Ophthalmology*, 67(1), 38.

https://doi.org/10.4103/ijo.ijo_568_18

- Shahzad, A., Köhler, G., Knapp, M., Gaubitzer, E., Puchinger, M., & Edetsberger, M. (2009). Emerging applications of fluorescence spectroscopy in medical microbiology field. *Journal of Translational Medicine*, 7(1). <https://doi.org/10.1186/1479-5876-7-99>
- Yang, H., Zhou, C., An, J., Yang, L., Yang, Y., & Liu, X. (2022). Ultra-fast synthesis of iron decorated multiwalled carbon nanotube composite materials: A sensitive electrochemical sensor for determining dopamine. *Journal of Alloys and Compounds*, 897, 163257. <https://doi.org/10.1016/j.jallcom.2021.163257>
- Yao Shen Chen, Zhang, X., Wang, A.-J., Zhang, Q.-L., Huang, H., & Feng, J.-J. (2019). Ultrafine Fe₃C nanoparticles embedded in N-doped graphitic carbon sheets for simultaneous determination of ascorbic acid, dopamine, uric acid and xanthine. 186(9). <https://doi.org/10.1007/s00604-019-3769-y>
- Zacharioudaki, D.-E., Ftilis, I., & Kotti, M. (2022). Review of Fluorescence Spectroscopy in Environmental Quality Applications. *Molecules (Basel, Switzerland)*, 27(15), 4801. <https://doi.org/10.3390/molecules27154801>
- Zakaria, H., Kurdi, R. E., & Patra, D. (2022). Curcumin-PLGA based nanocapsule for the fluorescence spectroscopic detection of dopamine. *RSC Advances*, 12(43), 28245–28253. <https://doi.org/10.1039/D2RA01679F>
- Zhang, H. and Liu, S. (2020). Electrochemical sensors based on nitrogen-doped reduced graphene oxide for the simultaneous detection of ascorbic acid, dopamine and uric acid.

Journal of Alloys and Compounds, [online] 842, p.155873.
doi:<https://doi.org/10.1016/j.jallcom.2020.155873>.